

Performance analysis on direct torque controlled induction motor drive with varying hysteresis controller bandwidth

S. Allirani¹, N. Subha Lakshmi², H. Vidhya³

¹Department of Electrical and Electronics Engineering, Sri Ramakrishna Engineering College, India

²Department of Electrical and Electronics Engineering, Sri Krishna College of Engineering and Technology, India

³Department of Electrical and Electronics Engineering, Sri Ramakrishna Engineering College, India

Article Info

Article history:

Received Aug 28, 2019

Revised Feb 4, 2020

Accepted Mar 20, 2020

Keywords:

Direct torque control
Flux vector estimation
Space vector modulation
Induction Motor

ABSTRACT

The foremost issue in DTC based induction motor drive is its torque ripples. The core objective of this paper is to reduce the electromagnetic torque ripples by varying the hysteresis controller bandwidth. Space Vector Modulation (SVM) based Direct Torque Controlled (DTC) induction motor drive is simulated in MATLAB/SIMULINK environment and its performance is studied with step change in load torque. The influence of hysteresis controller bandwidth on the performance of induction motor drive is analysed in terms of stator flux and electromagnetic torque ripples. The electromagnetic torque response and the stator flux trajectory for different values of hysteresis controller bandwidth are obtained and the results are presented.

This is an open access article under the [CC BY-SA](https://creativecommons.org/licenses/by-sa/4.0/) license.



Corresponding Author:

S. Allirani

Department of Electrical and Electronics Engineering,
Sri Ramakrishna Engineering College, Vattamalaipalayam,
Coimbatore, India.

Email: allirani.saminathan@srec.ac.in

1. INTRODUCTION

Variable speed AC drives are widely used in production plants like paper, cement, and textile mills etc, transportation systems, fans, pumps, blowers, wind generation systems, domestic electrical appliances etc. Electrical drives can be classified based on its source as AC drives and DC drives and as constant speed and variable speed drives depending on their mechanical output characteristics and applications. AC machines are basically constant speed and nearly constant speed machines and hence suitable for constant speed applications. DC machines can be used in variable speed applications as their speeds can be varied easily by simple means, which is not the case with AC machines. However, the DC machines suffer from many disadvantages like higher cost, weight and importantly, problems with commutator and its maintenance requirements. These disadvantages seemed to have outweighed its advantages, causing a spurt in research activities aiming to convert the constant speed induction motor into a variable speed AC drive. In majority of industrial environments, an induction motor is preferred due to its simple mechanical construction, reliability, ruggedness, low cost and low maintenance requirements. However, these advantages pale into insignificance when the motor is judged from control aspects. As induction motors are non-linear higher order systems of complexity, an advanced control technique and flexible controllers are required in order to extend the use of IM to variable speed applications. One such advanced control technique is Direct Torque Control (DTC), or Direct Self Control (DSC), introduced and developed by Takahashi & Naguchi in 1984 [1] and Depenbrock in 1988 [2].

In [3], the author adopted a space vector modulation-based DTC for IM. Further, performance evaluation of direct torque-controlled drive in the continuous PWM square wave transition region was discussed in [4]. In modern factories, variable frequency drives with high performance control permit high volume of automated production with superior product quality. One such a high-performance control technique is identified as direct torque control technique in induction motor drive [5, 6]. In DTC, the control variables are the motor torque and magnetizing flux and they can be controlled directly. In DTC, the speed accuracy is 0.1% without encoder. This is satisfying the accuracy requirement for 95% of industrial drives applications. A DTC drive using an encoder can achieve a speed accuracy of 0.01% [7]. The advantage with DTC is that it is characterized by the absence of PI regulators, coordinate transformations, current regulators and pulse width modulated signal generators. DTC also allows a good torque control during steady state as well as transient operating conditions. One major drawback with DTC is the production of torque ripples at low speed operations. Different approaches like band constrained voltage vector selection [8], a constant switching frequency torque controller [9, 10], unified flux and torque controller [11], fuzzy logic based control approach based on AI based controller [12, 13, 14] are suggested and elaborated to reduce the torque ripples.

Another important technique applied for reducing current ripples and torque pulsations during steady state is SVM technique. In SVM based DTC, the merits of DTC are preserved along with improved steady state operations [15]. In [16], the author proposed a sliding mode controller-based induction motor drive. SVM-DTC based IM drive in order to reduce the switching harmonics. SVM based DTC for torque ripple minimization is also reported in the literature [17]. In [18], the author reported another technique named predictive control to reduce flux and torque ripples in IM drives. In [19], modified DTC in sensorless drive is proposed by the author. Recent days, DTC with nine switch inverters is proposed to control two induction motors independently [20]. Improved performance on DTC based induction motor drive is also reported [21]. In addition to induction machines, DTC is employed to control Permanent Magnet Synchronous Motor [22].

In this paper, it is proposed that the reduction of torque pulsation is done by reducing the bandwidth of the hysteresis controller. The system is completely simulated in Matlab and the results are presented. Chapter 2 explained about SVM based DTC, chapter 3 presented the simulation results, chapter 4 discussed about the drive performance with varying stator flux controller bandwidth. Finally, the paper is concluded in chapter 4

2. SVM BASED DTC

The basic principle of DTC is to regulate electromagnetic torque and stator flux magnitude by the direct selection of a space vector and corresponding control signals.

The generic DTC scheme for a Voltage Source PWM inverter-fed IM drive is shown in Figure 1. This includes two controllers of hysteresis. The time duration of the active voltage vectors is imposed by the stator flux, which move along the reference trajectory, whereas the time duration of the zero voltage vectors determined by the torque controller which keep the motor torque in the predefined hysteresis tolerance band. The inverter switching state is chosen by the voltage vector selection block at each sampling time (S_a , S_b , S_c) which reduces the instantaneous flux and the torque errors [23].

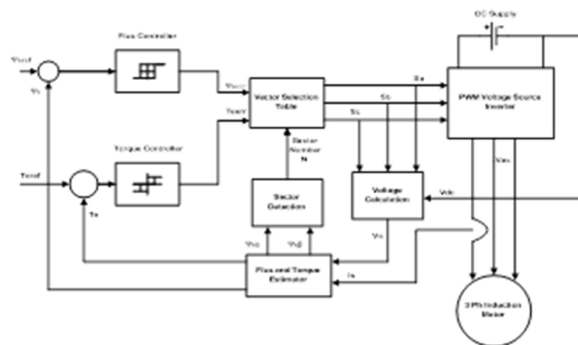


Figure 1. Generic scheme of PWM inverter fed induction motor with DTC

2.1. Basic switching table and selection of voltage vectors based on space vector modulation

The switching table of DTC concept is shown in Figure 1. The command stator flux Ψ_{sref} and T_{eref} values are compared with the actual Ψ_s and T_e values in hysteresis flux and torque controllers, respectively [23]. The digitized output signals of the flux controller are defined as in equations (1) and (2)

$$\psi_{serr} = 1, \text{ for } \psi_s < \psi_{sref} - H_\psi \quad (1)$$

$$\psi_{serr} = -1, \text{ for } \psi_s < \psi_{sref} + H_\psi \quad (2)$$

And those of the torque controller are as in (3), (4), (5),

$$T_{eerr} = 1, \text{ for } T_e < T_{eref} - H_m \quad (3)$$

$$T_{eerr} = 0, \text{ for } T_e = T_{eref} \quad (4)$$

$$T_{eerr} = -1, \text{ for } T_e < T_{eref} + H_m \quad (5)$$

Where $2H_\psi$ is the flux tolerance band and $2H_m$ is the torque tolerance band.

The digitized variables Ψ_{serr} , T_{eerr} and the stator flux sector (sector) N obtained from the angular position

$$\alpha = \arctg(\Psi_{s\beta} / \Psi_{s\alpha}) \quad (6)$$

Create a digital word which is used to select the appropriate voltage vector. The stator voltage space vector \bar{V}_s is calculated using the dc link voltage V_{dc} and the gating signals S_a , S_b , S_c as given in (7)

$$\bar{V}_s^s = \frac{2V_{dc}}{3} \left(S_a + e^{\frac{j2\pi}{3}} S_b + e^{\frac{j4\pi}{3}} S_c \right) \quad (7)$$

The SVM selects the inverter voltage vector from the Table 1 is done by depending on torque and flux hysteresis status and α . The outputs of the switching table are the settings for the switching devices of the inverter.

Table 1. Switching table of Inverter Voltage Vectors

Ψ_{serr}	T_{eerr}	$\alpha(1)sect1$	$\alpha(2)sect2$	$\alpha(3)sect3$	$\alpha(4)sect4$	$\alpha(5)sect5$	$\alpha(6)sect6$
1	1	V2	V3	V4	V5	V6	V1
	0	V7	V0	V7	V0	V7	V0
	-1	V6	V1	V2	V3	V4	V5
0	1	V3	V4	V5	V6	V1	V2
	0	V0	V7	V0	V7	V0	V7
	-1	V5	V6	V1	V2	V3	V4

2.2. Stator flux control

By selecting the suitable inverter output voltage V_i ($i=1-6$), the stator flux Ψ_s rotates at the desired frequency ω_s inside a specified band. If the stator ohmic drops are neglected, the stator voltage is given by equations (8) and (9).

$$\bar{V}_s = \frac{d\bar{\psi}_s}{dt} \quad (8)$$

$$d\bar{\psi}_s = \bar{V}_s dt \quad (9)$$

Thus the variation of the stator flux space vector due to the application of the stator voltage vector \bar{V}_s during a time interval of Δt can be approximated as in equation (10).

$$\Delta\bar{\psi}_s = \bar{V}_s \Delta t \quad (10)$$

As the stator flux linkage space vector move in the direction of the stator voltage space vector as long as the voltage space vector is applied. The aim is to keep the modulus of the stator flux linkage space vector $|\bar{\Psi}_s|$ within the hysteresis band, whose width is $2H_\psi$ as shown in Figure 2. The six sectors are shown

in Figure 2. The trajectory of the stator flux vector from P₀ to P₂ through P₁ can be explained in the following steps:

Step 1: Flux vector path from P₀ to P₁

It is assumed that initially the stator flux linkage space vector is at position P₀, in sector 1. If it is assumed that the stator flux vector is rotating anticlockwise, it follows that at position P₀, the stator flux vector is at the upper limit $|\bar{\Psi}_{sref}| + \Delta\bar{\Psi}_s$, and it must be reduced. This can be achieved by applying suitable switching vector. The corresponding switching vector is (0, 1, 0) which will provide V₃. Thus, the stator flux linkage space vector will move rapidly from point P₀ to point P₁ and it can be seen that P₁ is in sector 2 [24, 25].

2.3. Torque control

The electromagnetic torque given by equation (11) is a sinusoidal function of γ , the angle between Ψ_s and Ψ_r . The variation of stator flux vector will produce a variation in the developed torque because of the variation of the angle γ between the two vectors as in equation (12).

$$T_e = \frac{3}{2} \frac{P}{L_r L_s} \psi_s \psi_r \sin \gamma \tag{11}$$

$$\Delta T_e = \frac{3}{2} \frac{P}{L_r L_s} (\psi_s + \Delta\psi_s) \Psi_r \sin \Delta \gamma \tag{12}$$

Where $L_s' = L_s L_r - L_m^2$

2.4. Stator flux estimator

In the stationary reference frame, the d and q axes stator fluxes are estimated based on (13), (14).

$$\bar{\psi}_{ds} = \int (\bar{V}_{ds} - \bar{i}_{ds} R_s) dt \tag{13}$$

$$\bar{\psi}_{qs} = \int (\bar{V}_{qs} - \bar{i}_{qs} R_s) dt \tag{14}$$

$$\bar{\psi}_s = \sqrt{\bar{\psi}_{ds}^2 + \bar{\psi}_{qs}^2} \tag{15}$$

2.5. Electromagnetic Torque Estimation

From the estimated stator flux and current components the electromagnetic torque of the motor is calculated as in (16)

$$T_e = 3 \frac{P}{2} (\bar{\psi}_{ds} \bar{i}_{qs} - \bar{\psi}_{qs} \bar{i}_{ds}) \tag{16}$$



Figure 2. Trajectory of stator flux vector and inverter switching vectors

3. SIMULATION: RESULTS & DISCUSSIONS

The dynamic machine model in state space form is preferred in computer simulation for studying transient analysis of IM. From the voltages and machine parameters the state space model is obtained as in Equation (17), which is in the form of,

$$\frac{d}{dt}[X] = AX + BU$$

$$\frac{d}{dt} \begin{bmatrix} i_{ds} \\ i_{qs} \\ i_{dr} \\ i_{qr} \end{bmatrix} = \frac{1}{(L_m^2 - L_s L_r)} \begin{bmatrix} R_s L_r & -\omega L_m^2 & -R_r L_m & -\omega L_s L_m \\ \omega L_m^2 & R_s L_r & \omega L_s L_m & -R_r L_m \\ -R_r L_m & \omega L_s L_m & R_s L_r & \omega L_s L_m \\ -\omega L_s L_m & -R_r L_m & -\omega L_s L_m & R_s L_r \end{bmatrix} \begin{bmatrix} i_{ds} \\ i_{qs} \\ i_{dr} \\ i_{qr} \end{bmatrix} + \begin{bmatrix} -L_r & 0 \\ 0 & -L_r \\ L_m & 0 \\ 0 & L_r \end{bmatrix} \begin{bmatrix} v_{ds} \\ v_{qs} \end{bmatrix} \quad (17)$$

Initially the motor is started and allowed to operate under no-load condition. After sometime, at 0.4s instant a step change in load torque of 20 Nm is applied as input and the drive performance is studied from the response of three phase stator currents (i_{abc}), d and q axes stator currents (i_{ds} and i_{qs}), stator fluxes in d and q axes ψ_{ds} and ψ_{qs} , circular trajectory of stator flux, inverter output voltage, speed response, and estimated and observed electromagnetic torque. The d and q axes stator flux responses of SVM-DTC based IM drive are shown in Figure 3.

It is found that the two fluxes are independent to each other as they are orthogonal. The q axis flux is responsible for torque control whereas d axis flux is responsible for speed control. It is observed from the waveform that the stator flux distribution is almost sinusoidal. The circular trajectory of stator flux vector shown in Figure 3(b) is also proving the smooth sinusoidal distribution of stator flux which leads to smooth control of torque.

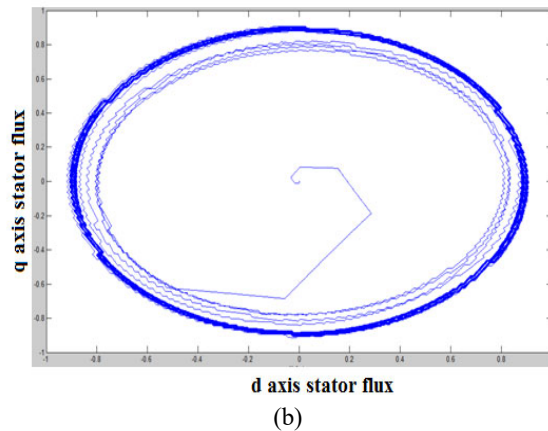
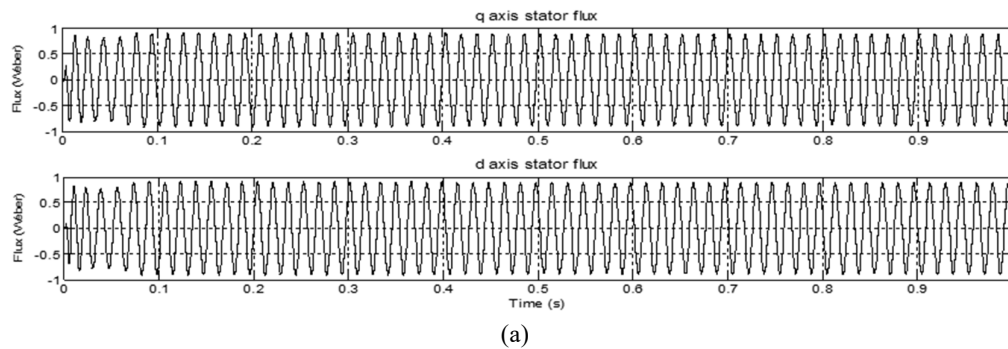


Figure 3. d and q axes stator fluxes of SVM – DTC based IM drive with step change in loadtorque at 0.4s
 (a) Actual d & q axes stator flux response; (b) Circular trajectory of stator flux

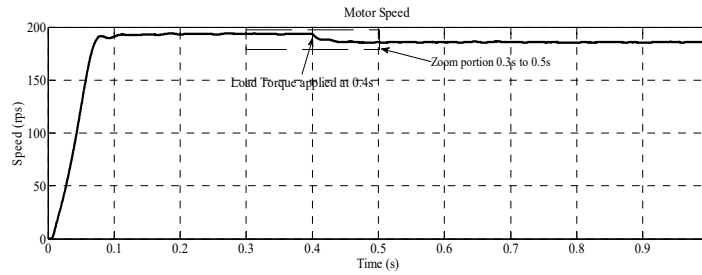


Figure 4. Speed response of SVM – DTC based IM drive with step change in load torque at 0.4s.

The speed response of SVM-DTC based IM drive with step change in load torque, applied at 0.4s is shown in Figure 4. As and when increase in load torque is applied, the speed of the drive proportionately reduced since the drive is operated in torque control mode. The torque response of SVM-DTC based IM drive when applying a step change in load torque is shown in Figure 5. It is observed that the electromagnetic torque tracks the reference torque immediately after applying load torque.

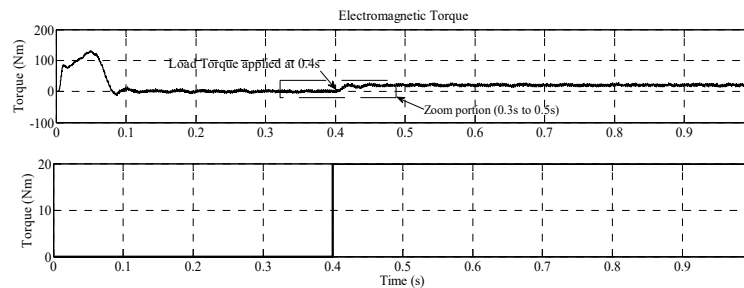


Figure 5. Torque response of SVM – DTC based IM drive with step change in load torque at 0.4s.

4. DRIVE PERFORMANCE WITH VARYING STATOR FLUX CONTROLLER BANDWIDTH

The steady state performance of the drive is studied by observing the ripple content in stator flux, stator current, electromagnetic torque responses and circular trajectory of stator flux vector for different values of hysteresis flux controller bandwidth.

4.1. Case i) Stator flux controller bandwidth tolerance: ± 0.1

The reference flux is set at 0.9 weber. The upper limit is set at $0.9+0.1 = 1$ weber, and lower limit is set at -1 weber. Then the responses of d and q axes stator currents, stator flux, electromagnetic torque and circular locus of stator flux are observed and are shown in Figure 6, Figure 7, Figure 8, Figure 9, and Figure 10.

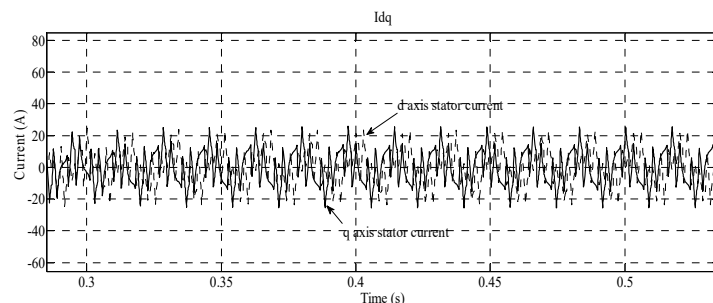


Figure 6. d and q axes stator currents with Fluxhysteresiscontroller bandwidth ± 0.1

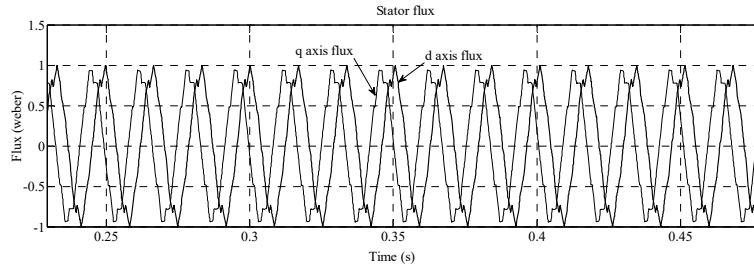


Figure 7. d and q axes stator fluxes with Flux hysteresis controller bandwidth ± 0.1

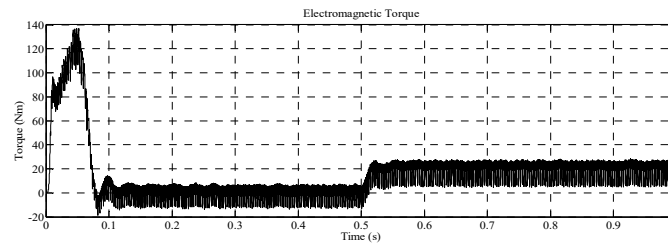


Figure 8. Torque response with Flux hysteresis controller bandwidth ± 0.1

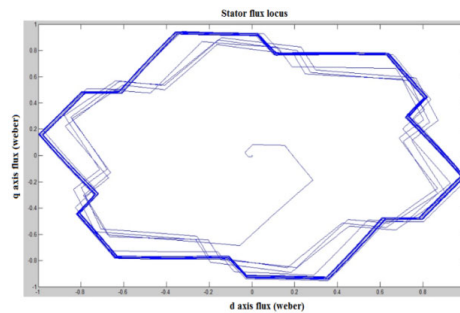


Figure 9. Locus of stator flux with flux hysteresis controller bandwidth ± 0.1

From these responses, it is observed that the ripple content in stator currents and fluxes and hence in torque responses is significant and are shown in Figure 10, Figure 11, Figure 12, and Figure 13. The stator flux vector locus follows hexagonal path instead of circular path.

4.2. Case ii) Stator flux controller bandwidth tolerance: ± 0.01

The reference flux is set as 0.9 weber. The upper limit is set at $0.9+0.01 = 0.91$ weber, and lower limit is set at -0.91 weber. Then the responses of d and q axes stator currents, stator flux, electromagnetic torque and circular locus of stator flux are observed for analysis. From the flux vector trajectory shown in Figure 10, it is understood that the stator flux vector significantly controls the ripple content.

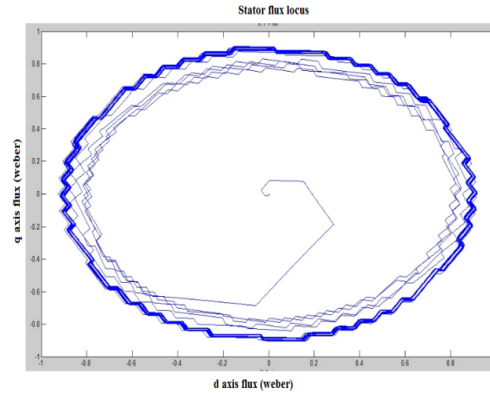


Figure10. Circular locus of stator flux with Fluxhysteresiscontroller

4.3. Case iii) Stator flux controller bandwidth tolerance: ± 0.001

The reference flux is set at 0.9 weber. The upper limit is set at $0.9+0.001 = 0.901$ weber, and lower limit is set at -0.901 weber. Then the responses of d and q axes stator currents, stator flux, electromagnetic torque and circular locus of stator flux are observed and are shown in Figures 11, Figure 12, Figure 13, and Figure 14 respectively.

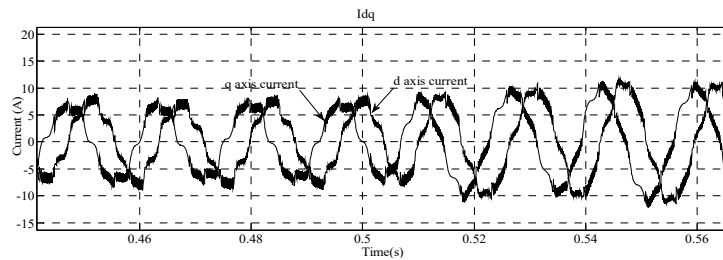


Figure 11. d and q axes stator currents with Fluxhysteresiscontroller bandwidth ± 0.001

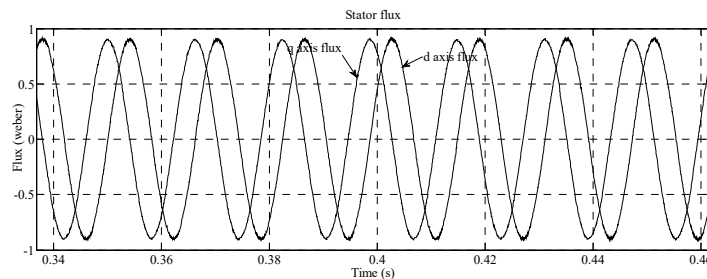


Figure 12. The d and q axes stator fluxes with Fluxhysteresiscontroller bandwidth ± 0.001

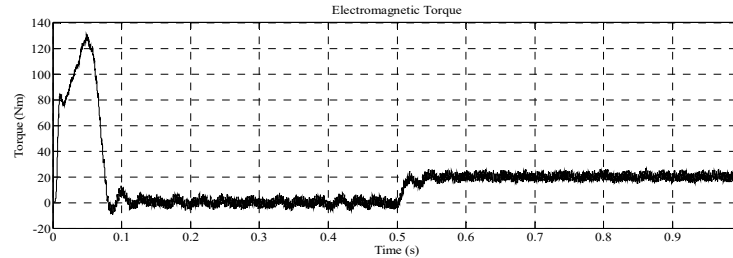


Figure 13. Electromagnetic torque response with Fluxhysteresis controller bandwidth ± 0.001

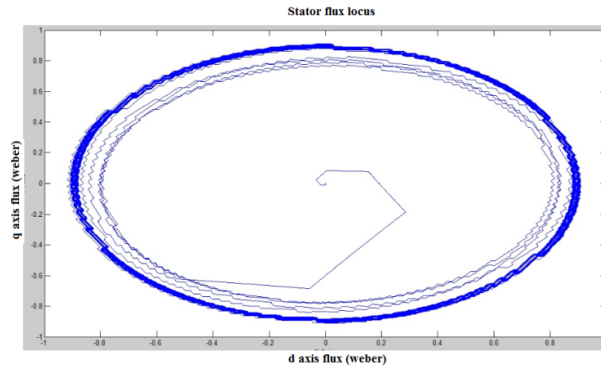


Figure 14. Circular locus of stator flux of with flux hysteresis controller bandwidth ± 0.001

From the results obtained for the above three different flux hysteresis controller tolerance bandwidths $H_\psi = 0.1$; $H_\psi = 0.01$ and $H_\psi = 0.001$, it is observed that the steady state performance of the drive in terms of oscillations on flux, current and hence torque is found better with $H_\psi = 0.001$. It is observed that the ripple content in torque response is significantly reduced when the flux band is adjusted [26].

5. CONCLUSIONS

In this paper, SVM based direct torque control of IM drive is re-examined for its merits. The concept of switching table and switching voltage vector selection based on SVM technique is reviewed and presented along with techniques for stator flux and electromagnetic torque estimations. The SVM-DTC based IM drive is modelled and simulated in MATLAB/SIMULINK environment and the drive performance is studied using simulation results. The drive performance is further studied for parameter variations. In this paper, the hysteresis controller band width is varied in steps and the corresponding drive performance is studied in MATLAB/SIMULINK environment. It is observed that by properly choosing the controller bandwidth, the torque ripples can be minimized.

REFERENCES

- [1] Takahashi, I and Noguchi, T, "A new quick response and high efficiency control strategy of an induction motor," *IEEE Transactions on Industry Applications*, vol. 1A-22, no. 5, pp. 820-827, 1986.
- [2] Depenbrock, M, "Direct Self Control (DSC) of inverter fed induction machine," *IEEE Transactions on Power Electronics*, vol. 3, no. 4, pp. 420-429, 1988.
- [3] Habetler, TG, Pastorelli, M, and Tolbert, L. M, "Direct torque control of induction machines using space vector modulation," *IEEE Transactions on Industry Applications*, vol. 28, no. 5, pp. 1045-1053, 1992.
- [4] Kazmierkowski, M. P and Kasprowicz, A. B, "Improved direct torque and flux vector control of PWM inverter fed induction motor drives," *IEEE Transactions on Industrial Electronics*, vol. 42, no. 4, pp. 344-350, 1995.
- [5] Allirani, S and Jagannathan, V, "Modeling and Simulation of High Performance Direct Torque Controlled Induction Motor Drive," *Journal of Electrical Systems (JES)*, vol. 9, no. 3, pp. 355-366, Sep 2013.
- [6] Allirani, S and Jagannathan, V, "Direct Torque Control Technique in Induction Motor Drives – A Review," *Journal of Theoretical and Applied Information Technology (JATIT)*, vol. 60, no. 3, pp. 452-472, Feb 2014.

- [7] Helsinki, "Direct torque control — the world's most advanced AC drive technology," *ABB Finland, Tech.Guide 1*, 1996.
- [8] Ambrozic, V. Buja, G.S, and Menis, R, "Band constrained technique for direct torque control of induction motor," *IEEE Transactions on industrial Electronics*, vol. 51, no. 1.4, pp. 776-784, 2004.
- [9] Idris, N.R.N.Halim, A and Yatim, M, "Direct torque control of induction machines with constant switching frequency and reduced torque ripple," *IEEE Transactions on Industrial Electronics*, vol. 51, no. 4, pp. 758-767, 2004.
- [10] Kang, J.K and Sul, S.K, "New direct torque control of induction motor for minimum torque ripple and constant switching frequency," *IEEE Transactions on Industry Applications*, vol. 35, no. 5, pp. 1076-1082, 1999.
- [11] Ryu, J.H. Lee, K.W and Lee, J.S, "A unified flux and torque control method for DTC based induction motor drives," *IEEE Transactions on Power Electronics*, vol. 21, no. 1, pp. 234-242, 1999.
- [12] Suddhir H, Kodad SF, and Survase, B, "Improved fuzzy logic based DTC of induction machine for wide range of speed control using AI based controller," *Journal of Electrical Systems*, vol. 12, no. 2, pp. 301-314, 2016.
- [13] Vengatashwara Rao V. M, Chandra Sekhar G and Obulesh Y.P, "Performance Comparison of PI and Fuzzy Logic Controllers of DTC for Torque ripple reduction," *International Journal of Engineering Research and Advanced Technology*, vol. 4, no. 01, pp. 1-18, Jan 2018.
- [14] Allirani, S and Jagannathan V, "Torque ripple minimization DTC based induction motor drive using fuzzy logic technique," *International Journal of Computer Applications*, vol. 40, no. 1, pp. 25-31, Feb 2012.
- [15] Baohua, L.Jianhua, Y and Weiguo, L, "Research on space vector modulation method for improving the torque ripple of direct torque control," *International Conference on computer design and Applications (ICCD 2010)*, pp. V3-502-V3-506, 2010.
- [16] Sun, D, "Sliding mode direct torque control for induction motor with robust stator flux observer," *International Conference on Intelligent Computation Technology and Automation, ICICTA, IEEE*, pp. 348-351, 2010.
- [17] Zelechowski, M.Kazmierkowski, M.P and Blaabjerg, F, "Controller design for direct torque controlled space vector modulated (DTC - SVM) induction motor drives," *IEEE, ISIE*, pp. 951-956, 2005.
- [18] Beerten, J.Vervecken, J and Drisen, J, "Predictive direct torque control for flux and torque ripple reduction," *IEEE Transactions on Industrial Electronics*, 2009.
- [19] Lascu, C.Boldea, I and Blaabjerg, F, "A modified direct torque control for induction motor sensor less drive," *IEEE Transactions on Industry Applications*, vol. 36, no. 1, pp. 122-130, 2000.
- [20] Draoui Abdelghani and AllaouaBoumodiene, "Direct torque control of two induction motors using the nine switch inverter," *International Journal of Power Electronics and drive system (IJPEDS)*, vol. 9, no. 4, pp. 1552-1564, Dec 2018.
- [21] Nour Mohamed, TedjiniHamza and GasbaouiBrahim, "Novel DTC induction machine drive improvement using controlled rectifier for DC voltage tuning," *International Journal of Power Electronics and Drive Systems*, vol. 10, no. 03, pp. 1223-1228, 2013.
- [22] Amir Yasim, Said Wahsh and M. Badr, "Cukoo Search based DTC of PMSM," *International Journal of Power Electronics and Drive System*, vol. 9, no. 03, pp. 1106-1115, Sep 2018.
- [23] Bimal. K. Bose, *Modern Power Electronics and AC- Drives*, PHI Learning Private Limited, 2002.
- [24] Boldea, I & Nasar, SA, '*Electric Drives*', Second Edition, Taylor & Francis, 2006.
- [25] Lazim, M.T.Muthanna, J.M.Alk-Khishali, Isa, A and Al-Shawi, "Space vector modulation direct torque speed control of induction motor," *ELSEVIER, Procedia Computer Science*, vol. 5, pp. 505-512, 2011.
- [26] Krishnan, R, *Electric Motor Drives- Modeling, Analysis, and Control*, Prentice-Hall of India, 2002.